PERGAMON

International Journal of Solids and Structures 36 (1999) 4225–4250

INTERNATIONAL JOURNAL OF SOLIDS and STRUCTURES

The stability analysis of a slider-crank mechanism due to the existence of two-component parametric resonance

Yi-Ming Wang

Division of Automobile Technology, Department and Graduate Institute of Industrial Education, College of Technology, National Chunghua Normal University, Chunghua, Taiwan

Received 31 July 1997; in revised form 20 June 1998

Abstract

The objective of this paper is an analytical and numerical study of the dynamics and dynamic instability of a slider-crank mechanism with an inextensible elastic coupler. Special attention is given to the phenomena arising due to modal interactions produced by the existence of multi-component, specifically two-component, parametric resonance. Such modal couplings are very common in the bending-bending motions of fixed/rotating beams. The two-component parametric resonance occurs when one of the natural frequencies of flexible parts of the mechanism is one-half or twice of the excitation frequency and simultaneously the sums or the differences among the internal frequencies are the same, or neighboring, as the frequency of excitation. The effects of two-component parametric resonance post on instability condition are also investigated. Resonance generated by more than two component modes are neglected due to its remote probability of occurrence in nature. The mechanics of the problem is Newtonian. Methods of analysis will consist of the dynamics of small deformations superimposed on the undeformed state. Without loss of generality and based on the Euler–Bernoulli beam theory, the coupled nonlinear equations of motion of a slider-crank mechanism with an inextensible flexible linkage are derived. The Newton's second law is used to obtain the boundary constraints at the piston end. Galerkin's procedure was used to remove the dependence of spatial coordinates in the partial differential equations. The method of multiple time scales is applied to consider the steady state solutions and the occurrence of dynamic instability of the resulting multidegree-of-freedom dynamical system with time-periodic coefficients.

1. Introduction

A great deal of work has been done on the problem of parametric excitations of mechanisms with flexible components. Typically due to the effect of inertia, these elastic links are subject to axial and transverse forces. The mathematical model of the problem then reduces to a system of coupled dynamic equations with time-periodic coefficients.

0020-7683/99/$ - see front matter
PII: S0020-7683(98)00198-X

Badlani and Kleinhenz (1979) discussed the dynamic stability of a slider-crank mechanism with an elastic connecting rod under the assumptions of Euler–Bernoulli and Timoshenko beam theories respectively. They pointed out that new regions of instability exist when the effect of rotary inertia and shear deformation are taken into account. Badlani and Midha (1982) analyzed the same manner except that the effect of initial curvature of the flexible link is involved. They developed a simple model that neglects the higher modes of vibrations and the interactions among amplitudes. Their results show that even a very small initial curvature of the coupler exists, the transient and steady-state solutions are amplified significantly.

Zhu and Chen (1983), and Jasinski et al. (1970) considered the problem of dynamic stability of a slider-crank mechanism with an elastic connecting rod. They assumed that the ratio of crank radius to the coupler is a small quantity. In the former paper, the authors applied perturbation method to the resulting equations of motion and obtained the Mathieu-type equations. Regions of dynamic instability then are determined on the basis of Mathieu equations. In the second paper, they employed the averaging method of Krylor and Bogoliubov to the equations of motion. The dynamic stability and steady state solutions are obtained from the resulting autonomous system.

Tadjbakhsh and Younis (1986) employed the Floquet theory to analyze the dynamic stability of a slider-crank mechanism with multi-links under the assumption of small deformations in the displacement field. They pointed out that the small deformation motion of each link is not influenced by the flexibility of other links. The individual stability criteria can be used to evaluate the overall dynamic stability of a flexible mechanism with multiple connecting rods.

Halbig and Beale (1995) carried out an experimental model to observe the dynamic responses of a flexible slider-crank mechanism at very high speed. They performed their experiments over a wide range of speeds as well as the crank length. They observed the occurrence of parametric resonance and determined regions of periodic doubling and amplified response.

Hsieh and Shaw (1994) analyzed the dynamic response and correspondingly the stability of a slider-crank by the method of multiple time scales. They discussed the phenomena produced by the occurrence of primary, superharmonic and subharmonic resonances. However, only single resonant mode was considered in their modeling.

It is known that the multi-component parametric resonance that exists depends not only on the parametric excitations but also on the commensurable relations of frequencies and the degrees of freedom of the system (Nayfeh and Mook, 1979). For a n degree-of-freedom coupled system with time-periodic coefficients, the existence of parametric resonance can have one or more components when one or more internal (natural) frequencies of the system and the excitation frequency are commensurable or nearly commensurable. The two-component parametric resonance then exists when one of the natural frequencies of flexible parts of the system is one-half or twice of the excitation frequency and simultaneously the sums or the differences of natural frequencies of the system are commensurable with the frequency of parametric excitation.

Results of present study indicate that the occurrence of two-component parametric resonance amplifies the region of instability and the possibility of existence of unstable motions. This is due to the modal interactions among modes and was not found in the analysis given by other authors (e.g. Badlani and Kleinhenz (1979), Hsieh and Shaw (1994)).

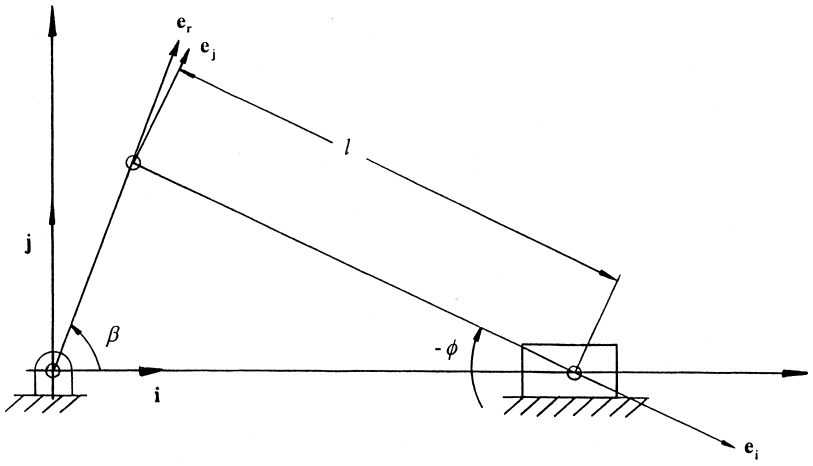

Fig. 1. System configuration.

2. Basic formulas

We consider a slider-crank mechanism with an inextensible initially straight elastic coupler as shown in Fig. 1. The mechanism consists of the rigid crank of radius r; the elastic link of length ℓ; a distributed mass, m, per unit length; and the frictionless piston of mass M.

In Fig. 1, the **i** and **j** represent the unit vectors of the Cartesian frame in the plane of the mechanism; $\mathbf{e}_i$ and $\mathbf{e}_j$ represent the unit vectors of the moving coordinate (x, y, z coordinates) system whose x ($\mathbf{e}_i$) coordinate is along the centroidal line of the straight elastic link; $\mathbf{e}_r$ is the unit vector along the crank. The position vector of point s along the link at time t is represented by $\mathbf{R}(s, t)$ and is given as

$$\mathbf{R}(s,t) = r\mathbf{e}_r + \mathbf{r} = r\mathbf{e}_r + (x(s) + u(s,t))\mathbf{e}_i + v(s,t)\mathbf{e}_j \tag{1}$$

where $u(s, t)$ and $v(s, t)$ are the axial and the transverse displacements of the rod from the dynamic undeformed state, respectively, and

$$\mathbf{e}_r = \cos(\beta-\phi)\mathbf{e}_i + \sin(\beta-\phi)\mathbf{e}_j = \cos\beta\mathbf{i} + \sin\beta\mathbf{j}$$

$$\mathbf{e}_i = \cos\phi\mathbf{i} + \sin\phi\mathbf{j}$$

$$\mathbf{e}_j = -\sin\phi\mathbf{i} + \cos\phi\mathbf{j}$$

where β is the angular displacement of the crank. The acceleration of points along the coupler in the moving coordinate system, $\mathbf{R}_{,tt}$, then is obtained from

$$\begin{aligned}\mathbf{R}_{,tt} = \frac{\mathrm{d}^2}{\mathrm{d}t^2}[\mathbf{R}(s,t)] = [&-r\beta_{,tt}\sin(\beta-\phi) - r\beta_{,t}^2\cos(\beta-\phi) + u_{,tt} - (x+u)\phi_{,t}^2 \\ &- 2v_{,t}\phi_{,t} - v\phi_{,tt}]\mathbf{e}_i + [r\beta_{,tt}\cos(\beta-\phi) - r\beta_{,t}^2\sin(\beta-\phi) + v_{,tt} + (x+u)\phi_{,tt} \\ &+ 2u_{,t}\phi_{,t} - v\phi_{,t}^2]\mathbf{e}_j \equiv a_x\mathbf{e}_i + a_y\mathbf{e}_j\end{aligned} \tag{2}$$

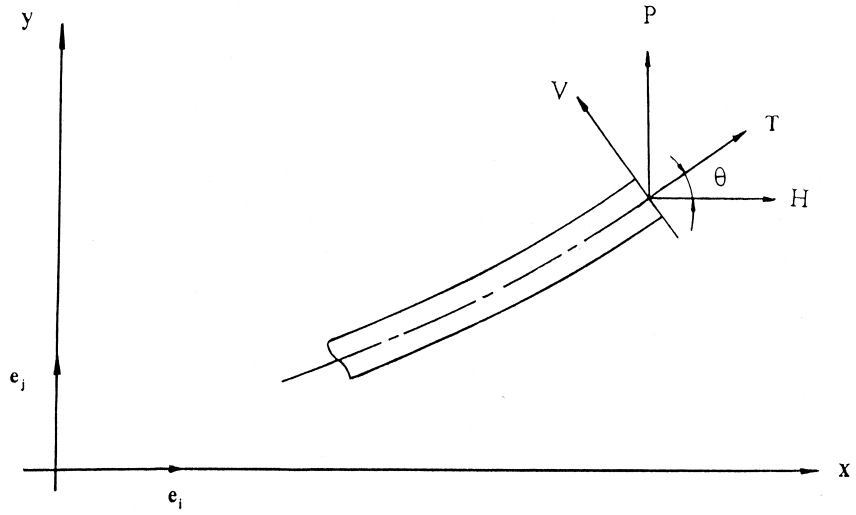

Fig. 2. Force equilibrium diagram.

where the subscript t denotes the time differentiation and

$$\sin(\beta-\phi) \approx \sin\beta+\frac{1}{2}\frac{r}{\ell}\sin 2\beta-\frac{1}{2}\left(\frac{r}{\ell}\right)^2\sin^3\beta$$

$$\cos(\beta-\phi) \approx \cos\beta-\frac{r}{\ell}\sin^2\beta-\frac{1}{2}\left(\frac{r}{\ell}\right)^2\cos\beta\sin^2\beta.$$

The angle ϕ and its time derivatives in the above equation can be eliminated from the following kinematic relationships (Viscomi et al. 1971):

$$\sin\phi = -\frac{r}{L}\sin\beta$$

$$\phi_{,t} = -\frac{r}{L}\beta_{,t}\cos\beta$$

$$\phi_{,tt} = \frac{r}{L}\beta_{,tt}^2\sin\beta-\frac{r}{L}\beta_{,tt}\cos\beta \tag{3}$$

The equations governing the motion of the system in the moving coordinate frame (x, y, z coordinates) can be derived from the dynamic equilibrium of forces and conservation of momenta. From Figs 1 and 2, one obtains

$$\mathbf{F}_{,s} = m\mathbf{R}_{,tt}, \quad 0 < s < \ell, \quad t > 0 \tag{4}$$

$$\bar{M}_{,s} + V = 0, \tag{5}$$

with the inextensibility constraint

$$\mathbf{r}_{,s} \cdot \mathbf{r}_{,s} = 1, \tag{6}$$

where the subscript s denotes the s differentiation. The force $\mathbf{F}$ is given by

$$\mathbf{F} = H\mathbf{e}_i + P\mathbf{e}_j = (T\cos\theta + V\sin\theta)\mathbf{e}_i + (T\sin\theta - V\cos\theta)\mathbf{e}_j \tag{7}$$

where T is the axial force in the coupler; V is the transverse force in the coupler; E and I are the Young's modulus and the area moment of inertia of the coupler respectively; and $\bar{M} = -EIv_{,ss}$. The unit tangent and normal vectors, τ and $\mathbf{n}$, to the coupler configuration are given by $\tau = (1+u_{,s})\mathbf{i} + v_{,s}\mathbf{j} = \cos\theta\mathbf{i} + \sin\theta\mathbf{j}$ and $\mathbf{n} = -v_{,s}\mathbf{i} + (1+u_{,s})\mathbf{j} = -sin\,\theta\mathbf{i} + \cos\theta\mathbf{j}$.

Substitution of eqns (2), (3), (5), and (7) into eqn (4), the equations of motion in directions $\mathbf{e}_i$ and $\mathbf{e}_j$ yield

$$[T(1+u_{,s}) + EIv_{,sss}v_{,s}]_{,s} = ma_x, \quad 0 < s < \ell, \quad t > 0, \tag{8}$$

$$[Tv_{,s} - EIv_{,sss}(1+u_{,s})]_{,s} = ma_y, \quad 0 < s < \ell, \quad t > 0 \tag{9}$$

where a_x and a_y are defined by eqn (2). Therefore, eqn (9) represents the motion of the linkage in the $\mathbf{e}_j$ direction and eqn (8) determines the axial force $T(s, t)$ of the coupler.

As shown in Fig. 1, two types of boundary conditions are stated. The first is that the coupler is assumed to be hinged at each end. Therefore, the longitudinal displacement vanishes at $s = 0$. The moment and transverse displacement vanish at $s = 0,\ell$. The second is when Newton's second law is employed to provide a force balance between the axial and shear forces of the rod and the inertia force of the frictionless piston (e.g. Badlani and Kleinhenz, 1979). The boundary conditions then are:

$$u(0,t) = v(0,t) = v(\ell,t) = \frac{\partial^2 v(0,t)}{\partial s^2} = \frac{\partial^2 v(\ell,t)}{\partial s^2} = 0 \tag{10}$$

$$(H + Ma_x)\cos\phi - (P + Ma_y)\sin\phi = 0 \quad \text{at} \quad s = \ell \tag{11}$$

From eqn (11), one obtains

$$T(\ell,\tau) \approx -Ma_x - EIv_{,sss}v_{,s} + \tan\phi(-EIv_{,sss} + Ma_y) \quad \text{at} \quad s = \ell \tag{12}$$

To determine the axial force $T(s, t)$, we integrate eqn (8) and use the boundary constraint, eqn (12). After some manipulations, the result yields

$$T(s,t) \times (1+u_{,s}) + EIv_{,sss}v_{,s} = \int_0^s ma_x \,\mathrm{d}s + C(t) \tag{13}$$

where $C(t)$ is constant of integration and is given by

$$C(t) = T(\ell,t) \times (1+u_{,s})|_{s=\ell} + EIv_{,sss}v_{,s}|_{s=\ell} - \int_0^\ell ma_x \,\mathrm{d}s$$

This result can be inserted into eqn (9).

The equations of motion of the slider-crank mechanism with constant angular velocity, $\hat{\omega} = \text{constant}$, in dimensionless form can be obtained by introducing the following dimensionless quantities:

$$\tau = \hat{\omega}t, \quad \hat{u} = \frac{u}{\ell}, \quad \hat{v} = \frac{v}{\ell}, \quad \xi = \frac{r}{\ell}, \quad \eta = \frac{s}{\ell},$$

$$\hat{I}_m = \frac{EI}{m\ell^4\hat{\omega}^2}, \quad \hat{I}_M = \frac{EI}{M\ell^3\hat{\omega}^2}, \quad \hat{M} = \frac{M}{m\ell} \tag{14}$$

Substitution of eqn (14) into eqn (9), one gets

$$\hat{v}_{,\tau\tau} + \hat{I}_m \frac{\partial^4 \hat{v}}{\partial \eta^4} - \xi^2(\cos^2\tau)\hat{v} - \frac{\partial T(\eta,\tau)}{\partial \eta}\frac{\partial \hat{v}}{\partial \eta} - T(\eta,\tau)\frac{\partial^2 \hat{v}}{\partial \eta^2} - 2\xi\cos\tau\hat{u}_{,\tau} + \xi\sin\tau\hat{u} = \xi\sin\tau(1-\eta) + \tfrac{1}{2}\xi^2\sin 2\tau - \tfrac{1}{2}\xi^3\sin^3\tau \tag{15}$$

where

$$\frac{\partial T(\eta,\tau)}{\partial \eta} = -\xi\cos\tau + 2\xi\cos\tau\hat{v}_{,r} - \xi\sin\tau\hat{v} + \xi^2[\sin^2\tau - (\cos^2\tau)\eta] + \frac{1}{2}\xi^3\cos\tau\sin^2\tau$$

and

$$T(\eta,\tau) = -\xi\cos\tau(\eta-1) + \hat{M}\xi\cos\tau - 2\xi\cos\tau\int_\eta^1 \hat{v}_{,\tau}\,\mathrm{d}\eta + \xi\sin\tau\int_\eta^1 \hat{v}\,\mathrm{d}\eta + \hat{I}_m\xi\sin\tau\hat{v}'''|_{\eta=1} + \xi^2\sin^2\tau(\eta-1) + \hat{M}\xi^2\cos 2\tau - \tfrac{1}{2}\xi^2\cos^2\tau(\eta^2-1) + \tfrac{1}{2}\xi^3\cos\tau\sin^2\tau(\eta-1) - \tfrac{1}{2}\xi^3\hat{M}\cos\tau\sin^2\tau + \tfrac{1}{2}\xi^3\hat{M}\cos\tau\sin 2\tau$$

Examination of the dynamics governed by eqn (15) is the main aim in this study.

We begin by representing $\hat{u}$ and $\hat{v}$ as continuous functions. Let

$$\hat{v} = \sum_{i=1}^{\infty} A_i(\tau)\sin i\pi\eta, \quad 0 < \eta < 1, \quad \tau > 0, \tag{16a}$$

$$\hat{u}(\eta,\tau) = -\frac{1}{2}\sum_{i=1}^{\infty}\sum_{k=1}^{\infty} A_i(\tau)A_k(\tau)R_{ik}(\eta) \tag{16b}$$

where

$$R_{ik}(\eta) = (i\pi)(k\pi)\int_0^\eta \cos i\pi\eta\cos k\pi\eta\,\mathrm{d}\eta$$

Thus, the boundary condition, eqn (10), and the constraint relation, eqn (6), are satisfied. Now, eqns (16a) and (16b) are substituted into the normal equation of motion, eqn (15), which yields

$$\sum_{i=1}^{\infty}[\ddot{A}_i + ((i\pi)^2\hat{I}_m - \xi^2\cos^2\tau)A_i]\sin i\pi\eta$$

$$
\begin{aligned}
&-2\xi\cos\tau\sum_{i=1}^{\infty}\sum_{k=1}^{\infty}[(\dot{A}_i(\tau)A_k(\tau)+A_i(\tau)\dot{A}_k(\tau)]R_{ik}(\eta)\\
&+\xi\sin\tau\sum_{i=1}^{\infty}\sum_{k=1}^{\infty}A_i(\tau)A_k(\tau)R_{ik}(\eta)-\frac{\partial T(\eta,\tau)}{\partial\eta}\sum_{i=1}^{\infty}(i\pi)A_i\cos i\tau\eta\\
&+T(\eta,\tau)\sum_{i=1}^{\infty}(i\pi)^2A_i\sin i\pi\eta\\
&=2\xi\sin\tau(1-\eta)+\xi^2\sin 2\tau-\xi^3\sin^3\tau\\
&\tau>0,\quad j=1,2,3,\ldots,(\dot{}\,)=\frac{\mathrm{d}}{\mathrm{d}\tau}
\end{aligned}
\tag{17}
$$

where $\partial T(\eta,\tau)/\partial\eta$ and $\mathrm{T}(\eta,\tau)$ in eqn (17) are given in the Appendix. It is mentioned here that in eqn (17) the terms higher than $\hat{v}^2$ are neglected by the assumption that $\hat{v}$ is a small quantity.

The approximate solution of the slider-crank mechanism is to be obtained by employing the Galerkin's method. Using Galerkin's procedure for minimizing error, we multiply eqn (17) by $\sin j\pi\eta$ and integrate eqn (17) with respect to η from 0 to 1, thus obtaining

$$
\begin{aligned}
&\ddot{A}_j(\tau)+(\omega_j^2-\xi^2\cos^2\tau)A_j(\tau)-2\xi\cos\tau\sum_{i=1}^{\infty}\sum_{k=1}^{\infty}[\dot{A}_i(\tau)A_k(\tau)+A_i(\tau)\dot{A}_k(\tau)]\hat{R}_{ikj}(\eta)\\
&+\xi\sin\tau\sum_{i=1}^{\infty}\sum_{k=1}^{\infty}A_i(\tau)A_k(\tau)\hat{R}_{ikj}(\eta)-2\sum_{i=1}^{\infty}(i\pi)\Bigg[-\xi\cos\tau\alpha_{ij}^{cs}A_i(\tau)\\
&+2\xi\cos\tau A_i(\tau)\sum_{k=1}^{\infty}\alpha_{ikj}^{css}\dot{A}_k(\tau)-\xi\sin\tau A_i(\tau)\sum_{k=1}^{\infty}\alpha_{ikj}^{css}A_k(\tau)\Bigg]\\
&-2\Bigg\{-\frac{1}{2}\xi\cos\tau(j\pi)^2(\hat{M}+1)A_j(\tau)+\xi\cos\tau\sum_{i=1}^{\infty}(i\pi)^2\alpha_{ij}^{\eta ss}A_i(\tau)\\
&+\frac{1}{2}(2\xi\cos\tau-\xi\sin\tau)(j\pi)^2A_j(\tau)\sum_{i=1}^{\infty}\frac{(-1)^i}{i\pi}A_i(\tau)\\
&+(2\xi\cos\tau-\xi\sin\tau)\sum_{i=1}^{\infty}\sum_{k=1}^{\infty}\frac{(k\pi)^2}{i\pi}\alpha_{ikj}^{css}\dot{A}_i(\tau)A_k(\tau)\Bigg]\\
&+\frac{1}{2}(j\pi)^2\hat{I}_m\xi\sin\tau A_j(\tau)\left(\sum_{i=1}^{\infty}(-1)^i(i\pi)^3A_i(\tau)\right)\Bigg\}\\
&-\xi\sin\tau\sum_{i=1}^{\infty}\sum_{k=1}^{\infty}\hat{R}_{ikj}A_i(\tau)A_k(\tau)+2\xi\cos\tau\sum_{i=1}^{\infty}\sum_{k=1}^{\infty}\hat{R}_{ikj}(\dot{A}_i(\tau)A_k(\tau)+A_i(\tau)\dot{A}_k(\tau))\\
&=\frac{2}{j\pi}\xi\sin\tau+\frac{2}{j\pi}[1-(-1)^j]\xi^2(\sin 2\tau-\xi\sin^3\tau),\tau>0,\quad j=1,2,3,\ldots,(\dot{}\,)=\frac{\mathrm{d}}{\mathrm{d}\tau}
\end{aligned}
\tag{18}
$$

where

$$\omega_j^2 = (j\pi)^4 \hat{I}_m \quad \text{and} \quad \hat{R}_{ikj}(\eta) = \int_0^1 R_{ik}(\eta) \sin j\pi\eta \, \mathrm{d}\eta.$$

The results of the integration of the cosine and sine functions in the above equation α_{ij}^{cs} and $\alpha_{ij}^{\eta ss}$ are given in the Appendix.

To analyze the system governed by eqn (18), we allow the response of the system to be small but finite. Thus, the method of multiple time scales can be used to predict the responses of the system. According to this method, we assume that the amplitude, $A_j(\tau)$, has the expansion (Nayfeh, 1979)

$$\begin{aligned}
&A_j(\tau;\varepsilon) = \varepsilon A_{1j}(\tau_0,\tau_1,\tau_2,\dots) + \varepsilon^2 A_{2j}(\tau_0,\tau_1,\tau_2,\dots) + \varepsilon^3 A_{3j}(\tau_0,\tau_1,\tau_2,\dots) + \cdots \\
&\tau_n = \varepsilon^n \tau, \quad n = 0,1,2,\dots \\
&\frac{\mathrm{d}}{\mathrm{d}\tau} = \frac{\partial}{\partial\tau_0} + \varepsilon\frac{\partial}{\partial\tau_1} + \varepsilon^2\frac{\partial}{\partial\tau_2} + \cdots \equiv D_0 + \varepsilon D_1 + \varepsilon^2 D_2 + \cdots \\
&\frac{\mathrm{d}^2}{\mathrm{d}\tau^2} \equiv D_0^2 + 2\varepsilon D_0 D_1 + \varepsilon^2(D_1^2 + 2D_0 D_2) + \cdots
\end{aligned} \tag{19}$$

where ε is a measure of the amplitude of the response and is small compared to unity.

For the purpose of studying the parametric resonance of the non-autonomous differential equations, we substitute (19) into the equation of motion, (18), and set $\xi = \varepsilon\hat{\xi}$. After manipulating these equations, we equate coefficients of equal power of ε and obtain to order one and two:

$$\varepsilon^1: \quad D_0^2 A_{1j} + \omega_j^2 A_{ij} = \frac{2}{j\pi}\hat{\xi}\sin\tau_0 \tag{20}$$

$$\begin{aligned}
\varepsilon^2: \quad D_0^2 A_{2j} + \omega_j^2 A_{2j} = {} & -2D_0 D_1 A_{1j} - \hat{\xi}\cos\tau_0 (j\pi)^2(\hat{M}+1)A_{1j} \\
& - 2\hat{\xi}\cos\tau_0 \sum_{i=1}^{\infty}(i\pi)\alpha_{ij}^{cs} A_{1j} + 2\hat{\xi}\cos\tau_0 \sum_{i=1}^{\infty}(i\pi)^2 \alpha_{ij}^{\eta ss} A_{1i} \\
& + \frac{2}{j\pi}[1-(-1)^j]\hat{\xi}^2 \sin 2\tau_0
\end{aligned} \tag{21}$$

It is shown in eqn (20) that unbounded oscillation occurs when the frequency ω_j is near 1. Therefore, in the following, the conditions considered are related to the cases when the natural frequency ω_j is away from 1.

From eqn (20), it is seen that the amplitude, A_{1j}, is harmonic in τ_0, and its solution can be represented as

$$A_{1j} = a_j \cos(\omega_j\tau_0 + \phi_j) + \frac{2\hat{\xi}}{(j\pi)(\alpha_j^2 - 1)}\sin\tau_0 \equiv a_j \cos\beta_j + \hat{\xi}\Lambda_j \sin\tau_0 \tag{22}$$

where $a_j = a_j(\tau_1,\tau_2,\dots)$ is the amplitude of response; $\phi_j = \phi_j(\tau_1,\tau_2,\dots)$ is the phase angle and $\Lambda_j = 2/(j\pi)(\omega_j^2 - 1)$.

To seek the solution of A_{2j} defined by (21), we substitute (22) into (21). After some manipulations, we obtain:

$$D_0^2 A_{2j} + \omega_j^2 A_{2j} = 2\omega_j[(D_1 a_j)\sin\beta_j + a_j(D_1\phi_j)\cos\beta_j]$$
$$-\tfrac{1}{2}\hat{\xi}(j\pi)^2(\hat{M}+1)a_j(\cos\beta_{1j}^{+}+\cos\beta_{1j}^{-}) - \hat{\xi}\sum_{i=1}^{\infty}[(i\pi)\alpha_{ij}^{cs} - (i\pi)^2\alpha_{ij}^{\eta ss}]a_i(\cos\beta_{1i}^{+}+\cos\beta_{1i}^{-})$$
$$-\hat{\xi}^2\left\{\frac{1}{2}j\pi)^2(\hat{M}+1)\Lambda_j + \sum_{i=1}^{\infty}[(i\pi)\alpha_{ij}^{cs} - (i\pi)^2\alpha_{ij}^{\eta ss}]\Lambda_i - \frac{2}{j\pi}[1-(-1)^j]\right\}\sin 2\tau_0 \tag{23}$$

where $\beta_{1j}^{+} = (\omega_j+1)\tau_0 + \phi_j$ and $\beta_{1j}^{-} = (\omega_j-1)\tau_0 + \phi_j$.

Nayfeh and Mook (1979) pointed out that a multidegree-of-freedom dynamic system with parametric excitation will experience multi-components parametric resonance when two or more internal frequencies and the excitation frequency are commensurable or nearly commensurable. For a dynamic system with finite degrees of freedom similar to that defined by (23), parametric resonance may exist when $\omega_m \approx \frac{1}{2}\Omega$, $\omega_n - \omega_m \approx \Omega (n > m)$, and $\omega_n + \omega_m \approx \Omega$. Here ω_m is the dimensionless internal frequency of the mth mode of vibration and Ω is the frequency of excitation.

For the purpose of studying the effects of multi-component parametric resonance to the motion of the slider-crank mechanism, we selected the following two sets of frequencies so that the two-component parametric resonance defined by eqn (23) exist. These are: (1) $\omega_m \approx \frac{1}{2}$ and $\omega_n - \omega_m \approx 1$, $n > m$, and (2) $\omega_m \approx 2$ and $\omega_n - \omega_m \approx 1$, $n > m$.

2.1. Case 1

For the case of two-component resonance when $\omega_m \approx \frac{1}{2}$ and $\omega_n - \omega_m \approx 1$, $n > m$.

In order to express the commensurable relations of ω_m to $\frac{1}{2}$ and $\omega_n - \omega_m$ to 1, the detuning parameters σ_m and σ_n are introduced:

$$\tfrac{1}{2} = \omega_m + \varepsilon\sigma_m \tag{24}$$

$$1 = \omega_n - \omega_m + \varepsilon\sigma_n. \tag{25}$$

where $\omega_n = (n/m)^2\omega_m$.

The relationship between σ_m and σ_n can be determined from eqns (24) and (25) which yield

$$\varepsilon\sigma_n = \left[3 - \left(\frac{n}{m}\right)^2\right]\omega_m + 2\varepsilon\sigma_m \equiv K_{mn}\omega_m + 2\varepsilon\sigma_m \tag{26}$$

For the differences of the arguments of the cosine and sine functions of unequal arguments we have

$$\beta_{1m}^{-} = (\omega_m - 1)\tau_0 + \phi_m = -(\omega_m\tau_0 + \phi_m) - 2(\sigma_m\tau_1 - \phi_m) \equiv -(\beta_m + 2\delta_m) \tag{27}$$

$$= (\omega_m + 1)\tau_0 + \phi_m = (\omega_n\tau_0 + \phi_n) + (\sigma_n\tau_1 + \phi_m - \phi_n) \equiv \beta_n - \delta_{mn} \tag{28}$$

and similarly

$$\beta_{1n}^{-} = (\omega_n - 1)\tau_0 + \phi_n = (\omega_m\tau_0 + \phi_m) - (\sigma_n\tau_1 + \phi_m - \phi_n) = \beta_m - \delta_{mn} \tag{29}$$

where $\delta_m = \sigma_m\tau_\Gamma - \phi_m$ and $\delta_{mn} = \sigma_n\tau_\Gamma + \phi_m - \phi_n$. Therefore $\delta_m = \delta_m(\tau_1, \tau_2, \dots)$ and $\delta_{nm} = \delta_{nm}(\tau_1, \tau_2, \dots)$ are two new phase angles. From the definition of σ_m and σ_n we have

$$D_1\phi_m = \sigma_m - D_1\delta_m \tag{30}$$

and

$$D_1\phi_n = \sigma_n + D_1\phi_m - D_1\delta_{mn} \tag{31}$$

Returning to (23) the solvability conditions are the vanishing of the secular terms. These number four, two from each component equation. These are respectively:

$$2\omega_m D_1 a_m + \hat{\xi}[\tfrac{1}{2}(m\pi)^2(\hat{M}+1) + f_{mm}]a_m \sin 2\delta_m - \hat{\xi} f_{nm} a_m \sin\delta_{nm} = 0 \tag{32}$$

$$2\omega_m a_m D_1\phi_m - \hat{\xi}[\tfrac{1}{2}(m\pi)^2(\hat{M}+1) + f_{mm}]a_m \cos 2\delta_m - \hat{\xi} f_{nm} a_n \cos\delta_{mn} = 0 \tag{33}$$

$$2\omega_n D_1 a_n + \hat{\xi} f_{mn} a_m \sin\delta_{mn} = 0 \tag{34}$$

$$2\omega_n a_n D_1\phi_n - \hat{\xi} f_{mn} a_m \cos\delta_{mn} = 0 \tag{35}$$

where $f_{nm} = [(n\pi)\alpha_{nm}^{cs} - (n\pi)^2\alpha_{nm}^{\eta ss}]$.

The main purpose of eqns (32)–(35) is to determine the response of motion in steady state and the regions of unstable motion.

To study the local stability of the fixed point and the steady state solutions, we represent the first order problem in the form

$$A_{1j} = H_j(\tau_1, \tau_2, \dots)\exp(\hat{i}\omega_j\tau_0) + \bar{H}_j(\tau_1, \tau_2, \dots)\exp(-\hat{i}\omega_j\tau_0) - \hat{i}\tfrac{1}{2}\hat{\xi}\Lambda_j(\exp(\hat{i}\tau_0) - \exp(-\hat{i}\tau_0)), \quad j = 1, 2, 3, \dots \tag{36}$$

where $\hat{i} = \sqrt{-1}$ and $\bar{H}_j$ is the complex conjugate of H_j. The relation between the amplitude a_j and the coefficient H_j can be obtained by comparing (22) and (36), whereby one finds

$$H_j = \tfrac{1}{2}a_j\exp(\hat{i}\phi_j), \quad j = 1, 2, 3, \dots \tag{37}$$

where a_j and ϕ_j are the amplitude and phase of the jth mode. Therefore, we rewrite eqns (32)–(35) as

$$4\omega_m\hat{i}(D_1 H_m) + 2\hat{\xi}\hat{f}_{mm}\bar{H}_m\exp(2\hat{i}\sigma_m\tau_1) - 2\hat{\xi}f_{nm}H_n\exp(-\hat{i}\sigma_n\tau_1) = 0 \tag{38}$$

$$4\omega_n\hat{i}(D_1 H_n) + 2\hat{\xi}f_{mn}H_m\exp(\hat{i}\sigma_n\tau_1) = 0 \tag{39}$$

where $\hat{f}_{mm} = \frac{1}{2}(m\pi)^2(\hat{M}+1) + f_{mm}$.

To determine the stability of two-component parametric resonance we follow the procedure outlined in Nayfeh and Mook (1979) and let

$$H_k = \tfrac{1}{2}(x_k - \hat{i}z_k)\exp(\hat{i}\theta_k\tau_1) = \tfrac{1}{2}(x_k - \hat{i}z_k)\exp(\hat{i}\varepsilon\theta_k\tau), \quad k = m, n. \tag{40}$$

Here x_k and z_k are real and

$$\theta_k = \frac{\mathrm{d}\phi_k}{\mathrm{d}\tau} \tag{41}$$

For the resonant case, we substitute eqn (40) with (41) into the resonant equations defined by eqns

(38) and (39) and separate the real and imaginary parts. After some manipulations, we obtain a set of resonant equations in terms of x_k and z_k. Now, if a small perturbation is superimposed on x_k and z_k ($k = m, n$) then we have

$$x_k = x_k^0 + \hat{x}_k$$
$$z_k = z_k^0 + \hat{z}_k \tag{42}$$

Here x_k^0, z_k^0, $\hat{x}_k$ and $\hat{z}_k$ are the fixed points and the disturbances respectively. The local stability of a fixed point with respect to a small perturbation for each resonant case hence can be determined by the eigenvalues λ which are given by the zero of the determinant of the perturbation equations.

Following the procedure mentioned above, we first substitute eqn (40) with (41) into eqns (38) and (39) and then substitute eqn (42) into the new set of equations and separate the real and imaginary parts. After some manipulations, we get

$$\hat{x}'_m + \theta_m \hat{z}_m + \frac{\hat{\xi}}{2\omega_m} \hat{f}_{mm} \hat{z}_m + \frac{\xi}{2\omega_m} f_{nm} \hat{z}_n = 0 \tag{43}$$

$$\hat{z}'_m - \theta_m \hat{x}_m + \frac{\hat{\xi}}{2\omega_m} \hat{f}_{mm} \hat{x}_m - \frac{\xi}{2\omega_m} f_{nm} \hat{x}_n = 0 \tag{44}$$

$$\hat{x}'_n + \theta_n \hat{z}_n - \frac{\hat{\xi}}{2\omega_n f_{mn} \hat{z}_m} = 0 \tag{45}$$

$$\hat{z}'_n - \theta_n \hat{x}_n + \frac{\hat{\xi}}{2\omega_n} f_{mn} \hat{x}_m = 0 \tag{46}$$

The local stability of a fixed point with respect to a small perturbation can be determined by the eigenvalues λ which are given by the zero of the determinant of the equations of (43) through (46). This determinant is given by

$$\begin{vmatrix} \lambda & \sigma_m + \frac{\xi}{2\omega_m} \hat{f}_{mm} & 0 & \frac{\xi}{2\omega_m} f_{nm} \\ -\sigma_m + \frac{\xi}{2\omega_m} \hat{f}_{mm} & \lambda & -\frac{\xi}{2\omega_m} f_{nm} & 0 \\ 0 & -\frac{\xi}{2\omega_n} f_{mn} & \lambda & \sigma_m + \sigma_n \\ \frac{\xi}{2\omega_n} f_{mn} & 0 & -(\sigma_m + \sigma_n) & \lambda \end{vmatrix} = 0 \tag{47}$$

where $\hat{f}_{mm} = \frac{1}{2}(m\pi)^2(\hat{M}+1) + f_{mm}$, $\theta_m = D_1\phi_m = \sigma_m$, and $\theta_n = D_1\phi_m = \sigma_m + \sigma_n$. Thus, the characteristic equation of (47) has the form

$$\lambda^4 + r_1\lambda^3 + r_2\lambda^2 + r_3\lambda + r_4 = 0 \tag{48}$$

where

$$
\begin{aligned}
r_1 &= 0 \\
r_2 &= \sigma_m^2 + (\sigma_m + \sigma_n)^2 - \frac{\hat{\xi}}{2\omega_m}\hat{f}_{mm} - \frac{\hat{\xi}^2}{2\omega_m\omega_n} f_{mn} f_{nm} \\
r_3 &= 0 \\
r_4 &= \left[\sigma_m(\sigma_m + \sigma_n) + \frac{\hat{\xi}^2}{4\omega_m\omega_n} f_{mn} f_{nm}\right]^2 - \left[\frac{\hat{\xi}}{2\omega_m} f_{mm}(\sigma_m + \sigma_n)\right]^2
\end{aligned} \tag{49}
$$

The solution of eqn (48) is $\lambda^2 = \frac{1}{2}[-r_2 \pm \sqrt{r_2^2 - 4r_4}]$. Therefore, the transition values corresponding to the roots of eqn (48) with the coefficients defined by (49) are $r_4 = 0$ or

$$
\sigma_m(\sigma_m + \sigma_n) \pm \frac{\hat{\xi}}{2\omega_m}\hat{f}_{mm}(\sigma_m + \sigma_n) + \frac{\hat{\xi}^2}{4\omega_m\omega_n} f_{mn} f_{nm} = 0 \tag{50}
$$

Multiplying eqn (50) by ε^2 and substituting eqn (26) with eqns (24) and (25) to eliminate $\varepsilon\sigma_n$ in eqn (50). After some manipulations, the result yields

$$
3(\varepsilon\sigma_m)^2 + \left\{K_{mn}\omega_m \pm \frac{3\varepsilon\hat{\xi}\hat{f}_{mm}}{2\omega_m}\right\}(\varepsilon\sigma_m) \pm \frac{\varepsilon}{2}\hat{\xi}\hat{f}_{mm}K_{mn} + \frac{\varepsilon^2\hat{\xi}^2}{4\left(\frac{n}{m}\right)^2\omega_m^2} f_{mn} f_{nm} = 0 \tag{51}
$$

It is noted here that in the absence of internal resonance, $K_{mn} = f_{mn} = f_{nm} = 0$, eqn (51) coincides with the result of Badlani and Kleinhenz (1979) for $\omega_m \cong \frac{1}{2}$. That is, they reduce to

$$
\varepsilon\sigma_m = \pm\frac{\varepsilon\hat{\xi}\hat{f}_{mm}}{2\omega_m} = \pm\frac{\varepsilon\hat{\xi}}{2\omega_m}\left[\frac{1}{2}(m\pi)^2\left(\hat{M} + \frac{1}{2}\right)\right] \tag{52}
$$

The transition values corresponding to the roots of (51) are

$$
\begin{aligned}
\varepsilon\sigma_m = \frac{1}{6}\Bigg[&-\left(K_{mn}\omega_m \pm \frac{3\varepsilon\hat{\xi}\hat{f}_{mm}}{2\omega_m}\right) \\
&\pm K_{mn}\omega_m\sqrt{1 \mp \frac{3\varepsilon\hat{\xi}\hat{f}_{mm}}{K_{mn}\omega_m^2} + \left(\frac{\varepsilon\hat{\xi}}{K_{mn}\omega_m}\right)^2\left[\left(\frac{3\hat{f}_{mm}}{2\omega_m}\right)^2 - \frac{3f_{mn}f_{nm}}{\left(\frac{n}{m}\right)^2\omega_m^2}\right]}\Bigg]
\end{aligned} \tag{53}
$$

Therefore, the transition curves that separate the stable and unstable motions of the system from $\omega_m = \frac{1}{2}$ and $\omega_n = (n/m)^2\omega_m$ in the $\varepsilon\omega$ plane then are given by

$$\omega_m = \tfrac{1}{2} - \varepsilon\sigma_m = \tfrac{1}{2} - \tfrac{1}{6}\left[-(\tfrac{1}{2}K_{mn} \pm 3\varepsilon\hat{\xi}\hat{f}_{mm}) \pm \frac{1}{2}K_{mn}\sqrt{1 \mp \frac{12\varepsilon\hat{\xi}\hat{f}_{mm}}{K_{mn}} + 12\left(\frac{\varepsilon\hat{\xi}}{K_{mn}}\right)^2\left(3\hat{f}_{mm}^2 - 4\frac{f_{mn}f_{nm}}{\left(\frac{n}{m}\right)^2}\right)}\right] \tag{54a}$$

$$\omega_n = \left(\frac{n}{m}\right)^2\omega_m = \left(\frac{n}{m}\right)^2\left\{\tfrac{1}{2} - \tfrac{1}{6}\left[-(\tfrac{1}{2}K_{mn} \pm 3\varepsilon\hat{\xi}\hat{f}_{nm}) \pm \frac{1}{2}K_{mn}\sqrt{1 \mp \frac{12\varepsilon\varepsilon\hat{\xi}\hat{f}_{mm}}{K_{mn}} + 12\left(\frac{\varepsilon\hat{\xi}}{K_{mn}}\right)^2\left(3\hat{f}_{mm}^2 - 4\frac{f_{mn}f_{nm}}{\left(\frac{n}{m}\right)^2}\right)}\right]\right\} \tag{54b}$$

2.2. Case 2

For the condition of two-component resonance if $\omega_m \approx 2$ and $\omega_n - \omega_m \approx 1$.
Similar to that done in Case 1, we let

$$2 = \omega_m + \varepsilon\sigma_m \tag{55a}$$

$$1 = \omega_n - \omega_m + \varepsilon\sigma_n \tag{55b}$$

where σ_m and σ_n are the detuning parameters and

$$\varepsilon\sigma_n = \left[\frac{3}{2} - \left(\frac{n}{m}\right)^2\right]\omega_m + \frac{1}{2}\varepsilon\sigma_m \equiv \hat{K}_{mn}\omega_m + \frac{1}{2}\varepsilon\sigma_m \tag{56}$$

Hence

$$\begin{aligned} 2\tau_0 &= \omega_m\tau_0 + \sigma_m\tau_1 \\ &= (\omega_m\tau_0 + \phi_m) + (\sigma_m\tau_1 - \phi_m) \equiv \beta_m + \delta_m \end{aligned} \tag{57}$$

Returning to eqn (23), the solvability conditions for the case when $\omega_{\mathrm{m}} \approx 2$ and $\omega_{\mathrm{n}} - \omega_{\mathrm{m}} \approx 1$ are

$$2\omega_m D_1 a_m - \hat{\xi}f_{nm}a_n \sin\delta_{mn} = \hat{\xi}^2\{[\tfrac{1}{2}(m\pi)^2(\hat{M}+1) + f_{mm}]\Lambda_m - \Lambda_m^*\}\cos\delta_m \tag{58}$$

$$2\omega_m a_m D_1\phi_m - \hat{\xi}f_{nm}a_n \cos\delta_{mn} = \hat{\xi}^2\{[\tfrac{1}{2}(m\pi)^2(\hat{M}+1) + f_{mm}]\Lambda_m - \Lambda_m^*\}\sin\delta_m \tag{59}$$

$$2\omega_n D_1 a_n + \hat{\xi}f_{mn}a_m \sin\delta_{mn} = 0 \tag{60}$$

$$2\omega_n a_n D_1\phi_n - \hat{\xi}f_{mn}a_m \cos\delta_{mn} = 0 \tag{61}$$

where $\Lambda_m^* = 2/m\pi[1-(-1)^{\mathrm{m}}]$. Similar as before, we rewrite eqns (58)–(61) as the form

$$4\omega_m \hat{i} D_1 H_m + 2\hat{\xi} f_{mm} H_n \exp(-\hat{i}\sigma_n \tau_1) = \hat{i}\hat{\xi}^2 (\hat{f}_{mm}\Lambda_m - \Lambda_m^*, \exp(\hat{i}\sigma_m \tau_1) \tag{62}$$

$$4\omega_n \hat{i} D_1 H_n + 2\hat{\xi} f_{mm} H_m \exp(\hat{i}\sigma_n \tau_1) = 0 \tag{63}$$

To determine the steady state solutions and correspondingly the local stability of the steady state solutions, we substitute eqn (40) with eqn (41) into eqns (62) and (63) and separate the real and imaginary parts and obtain

$$x'_m + \theta_m z_m - \frac{\hat{\xi}}{2\omega_m} f_{nm} z_n = \frac{\hat{\xi}^2}{2\omega_m}(\hat{f}_{mm}\Lambda_m - \Lambda_m^*) \tag{64}$$

$$z'_m - \theta_m x_m + \frac{\hat{\xi}}{2\omega_m} f_{nm} x_n = 0 \tag{65}$$

$$x'_n + \theta_n z_n - \frac{\hat{\xi}}{2\omega_n} f_{mn} z_m = 0 \tag{66}$$

$$z'_n - \theta_n z_n + \frac{\hat{\xi}}{2\omega_n} f_{mn} x_m = 0 \tag{67}$$

To determine the steady state solutions, we return to eqns (64)–(67) and set $x'_m = z'_m = x'_n = z'_n = 0$ and $x_k^2 + z_k^2 = a_k^2$, $k = m, n$. The result yields

$$\begin{aligned} a_m &= \frac{2\hat{\xi}^2(\hat{f}_{mm}\Lambda_m - \Lambda_m^*)\omega_n\theta_n}{4\omega_m\omega_n\theta_m\theta_n - \hat{\xi}^2 f_{mn} f_{nm}} \\ &= \frac{\hat{\xi}^2(\sigma_m + \sigma_n)(\hat{f}_{mm}\Lambda_m - \Lambda_m^*)}{2\omega_m\left[\sigma_m(\sigma_m + \sigma_n) - \hat{\xi}^2 \dfrac{f_{mn} f_{nm}}{4\omega_m\omega_n}\right]} \equiv \frac{\hat{\xi}^2(\sigma_m + \sigma_n)(\hat{f}_{mm}\Lambda_m - \Lambda_m^*)}{2\omega_m \Delta} \end{aligned} \tag{68}$$

$$a_n = \frac{\hat{\xi} f_{mn}}{2\omega_n\theta_n} a_m = \frac{\hat{\xi} f_{mn}}{2\omega_n(\sigma_m + \sigma_n)} a_m \tag{69}$$

where

$$\Lambda_m = \frac{2}{(m\pi)(\omega_m^2 - 1)}$$

and

$$\Delta = \sigma_m(\sigma_m + \sigma_n) - \hat{\xi}^2 \frac{f_{mn} f_{nm}}{4\omega_m\omega_n}.$$

The local stability of a fixed point with respect to a small perturbation then is determined by the zero of the determinant of eqns (64)–(67). This determinant is obtained by substituting eqn (42) into the above four equations. Therefore, we have

$$\begin{vmatrix} \lambda & \sigma_m & 0 & -\dfrac{\xi}{2\omega_m} f_{nm} \\ -\sigma_m & \lambda & \dfrac{\xi}{2\omega_m} f_{nm} & 0 \\ 0 & -\dfrac{\xi}{2\omega_n} f_{mn} & \lambda & \sigma_m + \sigma_n \\ \dfrac{\xi}{2\omega_n} f_{mn} & 0 & -(\sigma_m + \sigma_n) & \lambda \end{vmatrix} = 0 \tag{70}$$

where $\theta_m = \sigma_m$ and $\theta_n = \sigma_m + \sigma_n$. The characteristic equation of (70) is

$$\lambda^4 + \hat{r}_2 \lambda^2 + \hat{r}_4 = 0 \tag{71}$$

where

$$\hat{r}_2 = \sigma_m^2 + (\sigma_m + \sigma_n)^2 + \frac{\xi^2}{2\omega_m \omega_n} f_{mn} f_{nm}$$

$$\hat{r}_4 = \left[\sigma_m(\sigma_m + \sigma_n) - \frac{\xi^2}{4\omega_m \omega_n} f_{mn} f_{nm} \right]^2$$

Similarly, the solution of eqn (71) is $\lambda^2 = \frac{1}{2}[-\bar{r}_2 \pm \sqrt{\bar{r}_2^2 - 4\bar{r}_4}]$. Hence, the transition values corresponding to the roots of eqn (71) are $\hat{r}_4 = 0$ which implies

$$\sigma_m(\sigma_n + \sigma_n) - \frac{\xi^2}{4\omega_m \omega_n} f_{mn} f_{nm} = 0 \tag{72}$$

Note that eqn (72) is the same result as Δ defined by eqn (68). Therefore, unbounded solutions exist if $\Delta = 0$. Next, we multiply eqn (72) by ε^2 and substitute eqn (56) with eqns (55a) and (55b) into eqn (72) to eliminate $\varepsilon\sigma_n$ and obtain

$$\frac{3}{2}(\varepsilon\sigma_m)^2 + \hat{K}_{mn}\omega_m(\varepsilon\sigma_m) - \frac{\varepsilon^2 \hat{\xi}^2}{4\omega_m \omega_n} f_{mn} f_{nm} = 0 \tag{73}$$

Thus, the detuning parameter $\varepsilon\sigma_m$ corresponding to the roots of (73) are

$$\varepsilon\sigma_m = \frac{1}{3}\left[-\hat{K}_{mn}\omega_m \pm \hat{K}_{mn}\omega_m \sqrt{1 + \frac{3\varepsilon^2 \hat{\xi}^2 f_{mn} f_{nm}}{2\hat{K}_{mn}^2 \omega_m^3 \omega_n}} \right] \tag{74}$$

The curves that unbounded motions of the system occur from $\omega_m = 2$ and $\omega_n = (n/m)^2 \omega_m$ in the $\xi\omega$ plane then are given by

$$\omega_m = 2-\varepsilon\sigma_m = 2-\frac{2}{3}\left[-\hat{K}_{mn} \pm \hat{K}_{mn}\sqrt{1+\frac{3\varepsilon^2\hat{\xi}^2 f_{mn}f_{nm}}{32\left(\frac{n}{m}\right)^2\hat{K}_{mn}^2}}\right] \tag{75}$$

$$\omega_n = \left(\frac{n}{m}\right)^2\omega_m = \left(\frac{n}{m}\right)^2(2-\varepsilon\sigma_m)$$

$$= \left(\frac{n}{m}\right)^2\left\{2-\frac{2}{3}\left[-\hat{K}_{mn} \pm \hat{K}_{mn}\sqrt{1+\frac{3\varepsilon^2\hat{\xi}^2 f_{mn}f_{nm}}{32\left(\frac{n}{m}\right)^2\hat{K}_{mn}^2}}\right]\right\} \tag{76}$$

3. Numerical results and discussions

Without loss of generality and considering the commensurable relations among frequencies and the probability of occurrence in nature we selected the following sets of commensurable relations of vibrating modes to determine the basic characteristics of the occurrence of two-component parametric resonance. For the case of $\omega_m \cong \frac{1}{2}$ and $\omega_n-\omega_m \cong 1$ we chose $m = 1$ and $n = 2$ to present the occurrence of two-component parametric resonance. For the condition that $\omega_m \cong 2$ and $\omega_n-\omega_m \cong 1$ we selected $m = 3$ and $n = 4$. It is recalled that the parameter ξ is the crank ratio; ω_j is the dimensionless natural frequency and is defined by

$$\omega_j = (j\pi)^2\sqrt{\frac{EI}{ml^4\hat{\omega}^2}}$$

where $\hat{\omega}$ is the constant angular velocity of the crank.

In addition to the stability analysis, the existence of perturbation solutions is verified by numerically integrating the modulation equations by the Runge-Kutta method with sixth order accuracy.

In the following figures, Figs 3–7 are related to the case when $\omega_1 \cong \frac{1}{2}$ and $\omega_2 = 4\omega_1$. The solid and chain-dot lines in these figures denote respectively the first and second modes of vibrations. The dash lines represent the first vibrating mode under the condition of one-component parametric resonance, $\omega_1 \cong \frac{1}{2}$. As mentioned previously, the validity of the model is verified by numerically integrating the modulation equations, eqns (32)–(35).

Figure 3 presents the transition curves that separate the regions of bounded (stable) and unbounded (unstable) motions emanating from $\omega_1 = \frac{1}{2}$ and $\omega_2 = 4\omega_1$ in the $\xi\omega$ parameter plane for $\hat{M} = 0.5$, where the shaded area denotes the region of unstable motion for the first vibrating mode. It is interesting that in this case, unbounded solutions almost always exist when the frequency of first mode is smaller than one-half of the excitation frequency, except a tiny region of small crank ratio. The occurrence of this new region of instability is, perhaps, due to the variation of energy between modes. The existence of bounded and unbounded solutions is evident in Figs 4–8.

Figure 4 shows the long-time behavior of the amplitude a_1 for $\hat{M} = 0.5$ and $\omega_1 = 0.3$ with two different values of crank ratio, $\xi = 0.02$ and $\xi = 0.025$. The lower plot in Fig. 4 is related to the

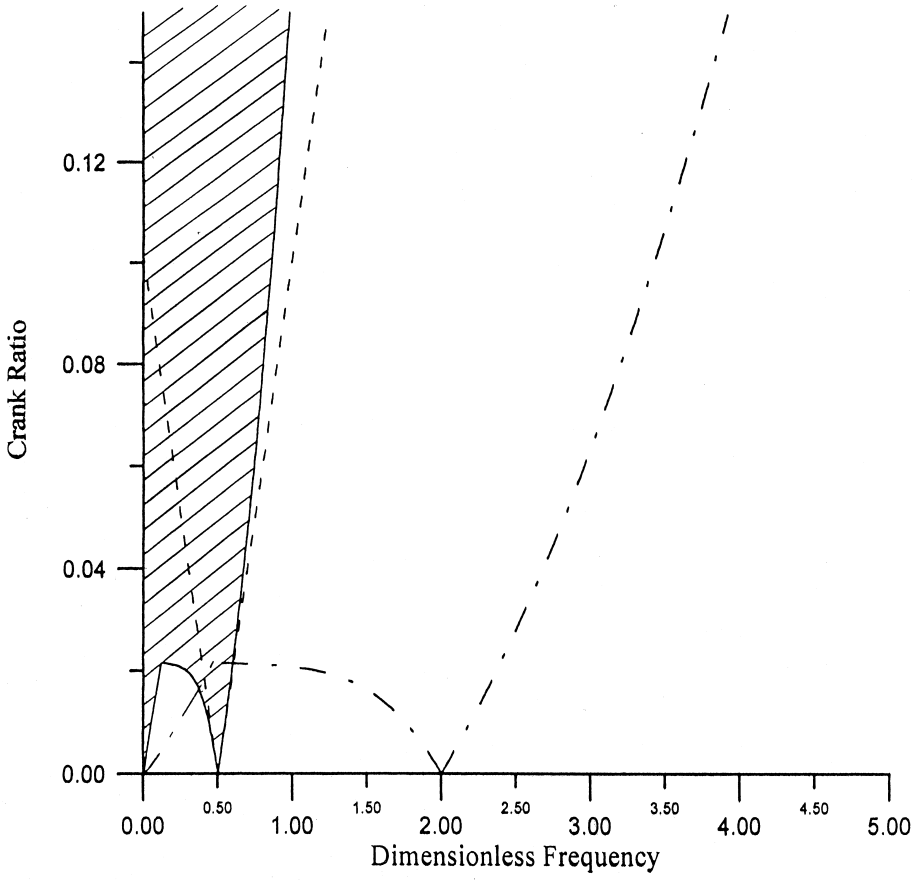

Fig. 3. Transition curves emanating from $\omega_1 = 1/2$ and $\omega_2 = 4\omega_1$ in the $\xi\omega$ plane for $\hat{M} = 0.5$.

case when $\xi = 0.02$ is encountered. The result clearly indicates the existence of bounded ($\xi = 0.02$) and unbounded ($\xi = 0.025$) solutions. Figure 5 illustrates similar information to that shown in Fig. 4, except that in Fig. 5, ω_1 is set to be 0.08 with $\xi = 0.015$ (lower plot) and $\xi = 0.08$ (upper plot). The result evidently shows in the case of two-component parametric resonance unstable motion may occur even the fundamental frequency is far less than the excitation frequency. This event was not found in the condition of one-component parametric resonance.

Figure 6 illustrates the time history of the amplitude a_1 for $\hat{M} = 0.5$ and $\omega_1 = 0.75$. In the lower plot ξ is set to be 0.05. In the top plot ξ is chosen to be 0.08. It evidences that the transition curves separate the bounded ($\xi = 0.05$) and unbounded ($\xi = 0.08$) motions of the system.

The transition curves emerging from $\omega_1 = \frac{1}{2}$ and $\omega_2 = 4\omega_1$ in the $\xi\omega$ parameter plane for $\hat{M} = 1.0$ is shown in Fig. 7. Figure 7 and Fig. 1 illustrate that it is generally true that the piston mass ratio $\hat{M}$ and the crank ratio ξ enlarge the regions of instability. In addition, the lower bound of the transition values of frequency diminishes as the piston mass ratio increases. In other words, under

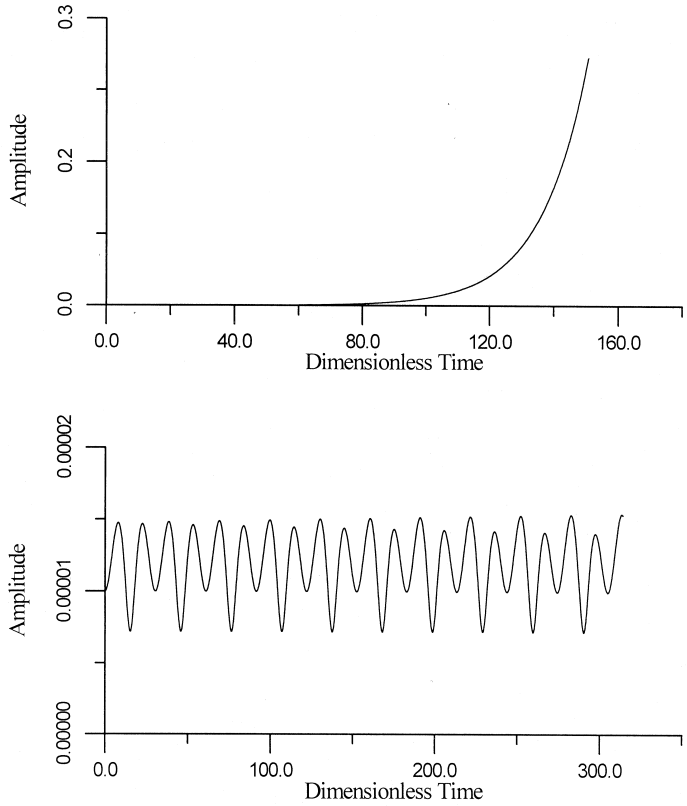

Fig. 4. Time history of the amplitude a_1 for $\omega_1 = 0.3$, $\hat{M} = 0.5$ and $\xi = 0.02$ (bottom plot) and $\xi = 0.025$ (top plot).

certain conditions, the motion of the system may become fully unstable when the fundamental frequency is lower than one-half of the excitation frequency.

In the following, the numerical study of solutions for the case when $\omega_3 \cong 2$ and $\omega_2 = 4\omega_1$ is carried out to determine some of the characteristics of response in steady state.

From eqn (69), we find that unbounded solutions exist if $\Delta = 0$. Hence, boundaries of the unstable solutions, as functions of the detuning parameter $\varepsilon\sigma_m$, $m = 3$, must be determined. We recall

$$a_m = \frac{\hat{\xi}^2(\sigma_m+\sigma_n)(\hat{f}_{mm}\Lambda_m - \Lambda_m^*)}{2\omega_m\left[\sigma_m(\sigma_m+\sigma_n) - \hat{\xi}^2\dfrac{f_{mn}f_{nm}}{4\omega_m\omega_n}\right]} \equiv \frac{\hat{\xi}^2(\sigma_m+\sigma_n)(\hat{f}_{mm}\Lambda_m - \Lambda_m^*)}{2\omega_m\Delta} \tag{68}$$

Therefore, unbounded solution exists if $\Delta = 0$ which implies

$$\frac{3}{2}(\varepsilon\sigma_m)^2 + \hat{K}_{mn}\omega_m(\varepsilon\sigma_m) - \frac{\varepsilon^2\hat{\xi}^2}{4\omega_m\omega_n}f_{mn}f_{nm} = 0$$

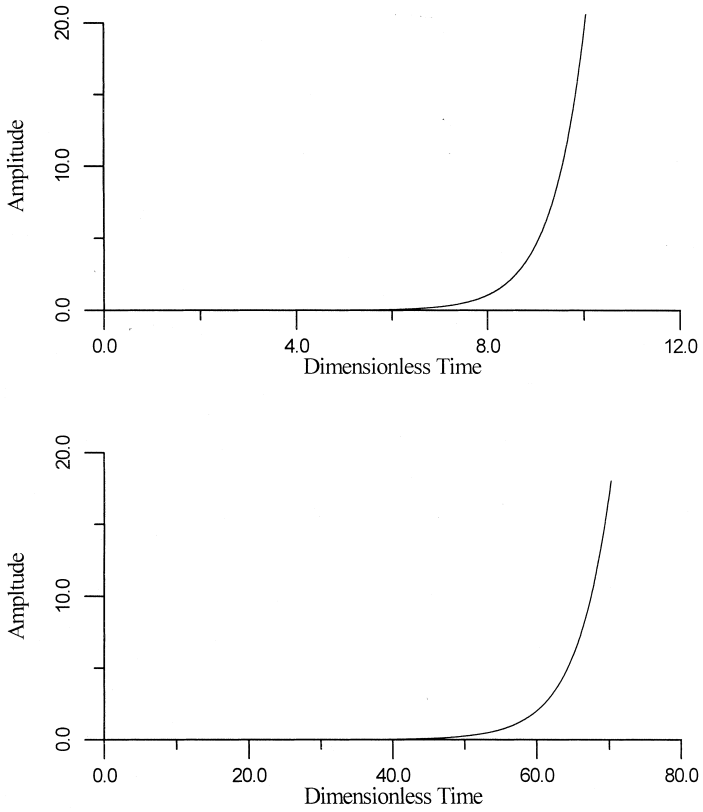

Fig. 5. Time history of the amplitude a_1 for $\omega_1 = 0.08$, $\hat{M} = 0.5$ and $\xi = 0.015$ (lower plot) and $\xi = 0.08$ (upper plot).

or

$$\xi = \varepsilon\hat{\xi} = \frac{2\left(\frac{n}{m}\right)\omega_m}{\sqrt{f_{mn}f_{nm}}}\sqrt{\frac{3}{2}(\varepsilon\sigma_m)^2 + \hat{K}_{mn}\omega_m(\varepsilon\sigma_m)} \tag{77}$$

where $|f_{mn}f_{nm}| > 0$. Note that in the above equation ξ is the crank ratio and has to be no less than zero which implies

$$(\varepsilon\sigma_m)[\tfrac{3}{2}(\varepsilon\sigma_m) + \hat{K}_{mn}\omega_m] \geqslant 0 \tag{78}$$

The result of eqn (78) yields the following two sets of solutions:

(1) $\varepsilon\sigma_m \geqslant 0$ and $\varepsilon\sigma_m \geqslant -\frac{2}{3}\hat{K}_{mn}\omega_m$.

(2) $\varepsilon\sigma_m \leqslant 0$ and $\varepsilon\sigma_m \leqslant -\frac{2}{3}\hat{K}_{mn}\omega_m$.

From the definition of $\hat{K}_{mn}$, $\hat{K}_{mn} = 3/2 - (n/m)^2$ (eqn (56)), we substitute $m = 3$ and $n = 4$ into $\hat{K}_{mn}$ and get $\hat{K}_{34} < 0$. Therefore, the occurrence of unbounded solutions exists if either $\varepsilon\sigma_3 \leqslant 0$ or

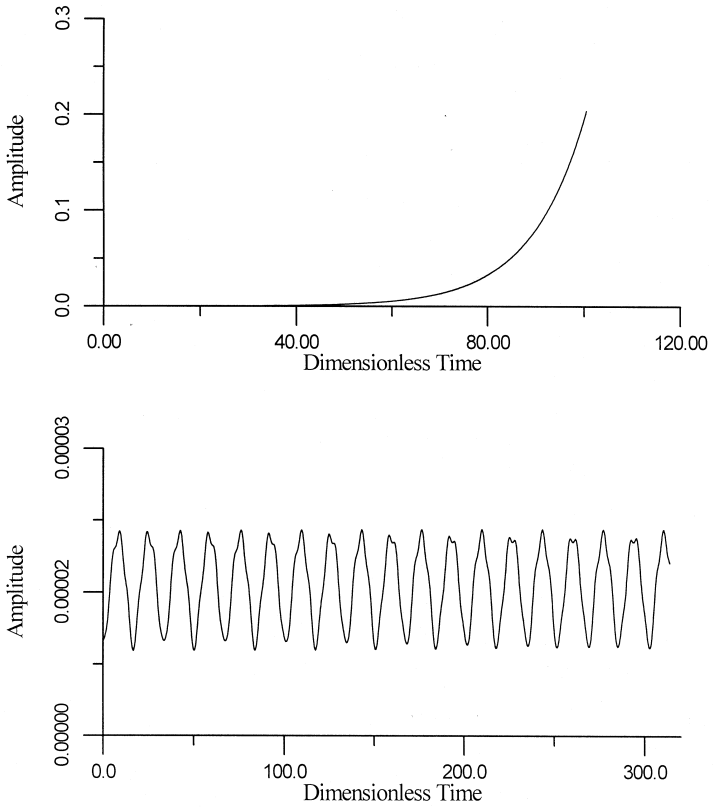

Fig. 6. Time history of the amplitude a_1 for $\omega_1 = 0.75$, $\hat{M} = 0.5$ and $\xi = 0.05$ (bottom plot) and $\xi = 0.08$ (top plot).

$\varepsilon\sigma_3 \geqslant -4/3\,\hat{K}_{34}$. Note that in the case of one-component parametric resonance unbounded solution occurs only when the detuning parameter $\varepsilon\sigma_3$ is zero. In addition, it is mentioned here that from eqn (77), we observed that the occurrence of unstable solutions is independent of the piston mass ratio $\hat{M}$.

Figure 8 shows the variations of the crank ratio ξ with the detuning parameter $\varepsilon\sigma_3$. In this figure, the solid line denotes the values of corresponding parameters such that the unstable solution occurs. As an example, if the crank ratio ξ is chosen to be 0.1 then unstable motion of the system exists when $\varepsilon\sigma_3$ is near either -0.066 or 0.426. If ξ is set to be 0.2 unbounded solution occurs when $\varepsilon\sigma_3$ is close to -0.192. This is verified in Figs 9 and 10.

Figure 9 shows the manner in which the amplitude a_3 is plotted with the detuning parameter $\varepsilon\sigma_3$ for $\xi = 0.1$ and clearly indicates unbounded solutions occur when the detuning parameter $\varepsilon\sigma_3$ is close to -0.066 and 0.426. As mentioned previously, the response of the system becomes unlimited when the internal frequency is equal to one. Therefore, unbounded solution exists when the detuning parameter $\varepsilon\sigma_3$ is close to one.

Figure 10 presents the long-time behavior of the amplitude a_3 for $\xi = 0.2$ and $\hat{M} = 0.5$ with two different values of detuning parameter $\varepsilon\sigma_3$. The lower one is related to the case when $\varepsilon\sigma_3 = -0.192$

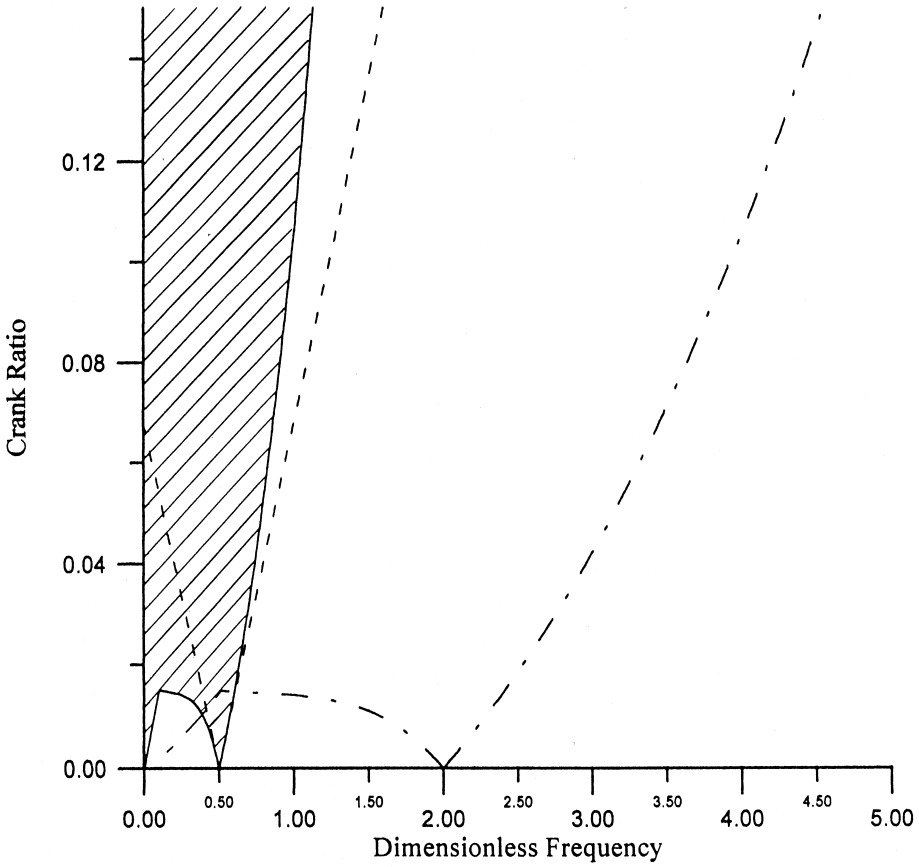

Fig. 7. Transition curves emanating from $\omega_1 = 1/2$ and $\omega_2 = 4\omega_1$ in the $\xi\omega$ plane for $\hat{M} = 1.0$.

and the upper one is connected to the case when $\varepsilon\sigma_3 = -0.4$. The results evidently show the existence of unbounded (upper plot) and bounded solutions.

The variation of amplitude a_3 with the crank ratio ξ for $\varepsilon\sigma_3 = 0.2$ ($\omega_3 = 1.8$) is shown in Fig. 11, where the solid line denotes $\hat{M} = 0.5$ and the dashed line is related to $\hat{M} = 1.0$. The existence of the amplitude in Fig. 11 is verified by the time history of solution for selected parameters, $\hat{M} = 1.0$ and $\xi = 0.13$, and is given by Fig. 12.

4. Conclusions

In this study, the weak form of the occurrence of two-component parametric resonance are obtained. The mechanics of a slider-crank mechanism and the phenomena produced by the existence of two-component parametric resonance are studied.

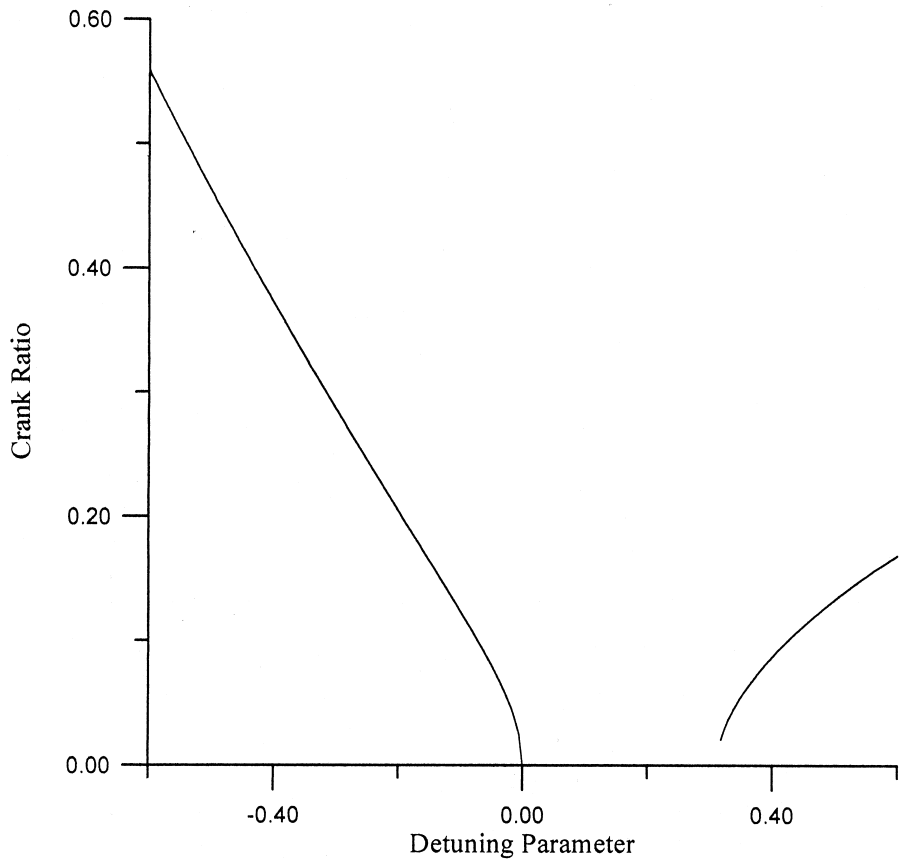

Fig. 8. The curves of unstable solutions emanating from $\omega_3 = 2$ in the $\xi - \varepsilon\sigma_3$ plane.

Results of the study show that for the case of one-component parametric resonance, which is a special case of the two-component model, regions of instability coincide with the linear result as reported by other authors (e.g. Badlani and Kleinhenz (1979)). However, in the condition of two-component resonance, new regions of instability of solutions are found (e.g. Figs 3 and 8). This is due to modal interactions caused by the existence of two-component parametric resonance.

For the case of two-component parametric resonance under the condition when one of the natural frequencies of the system is near twice of the excitation, higher vibrating modes, the existence of unstable motion of the system varies with the crank ratio (Fig. 8). However, this phenomenon was not able to be observed in the one-component parametric resonance (single mode condition). In that case, unbounded motion occurs only when the detuning parameter $\varepsilon\sigma_3$ is equal to zero (eqn (68) with $m = 3$, $\sigma_n = f_{mn} = f_{nm} = 0$). In addition, the result also shows that the mass ratio of the slider plays no effect to the occurrence of unstable motion.

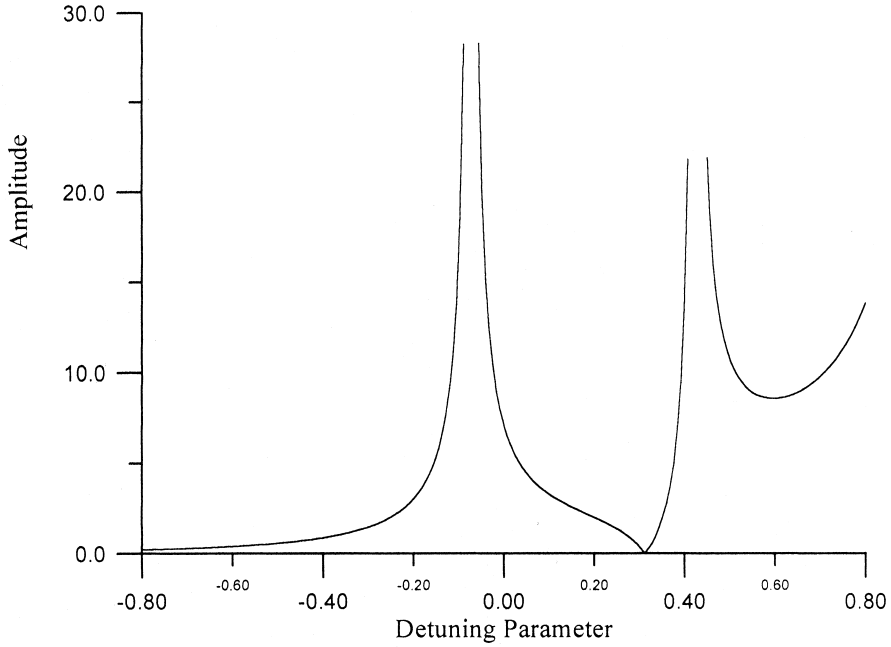

Fig. 9. The amplitude a_3 vs the detuning parameter $\varepsilon\sigma_3$ for $\xi = 0.1$.

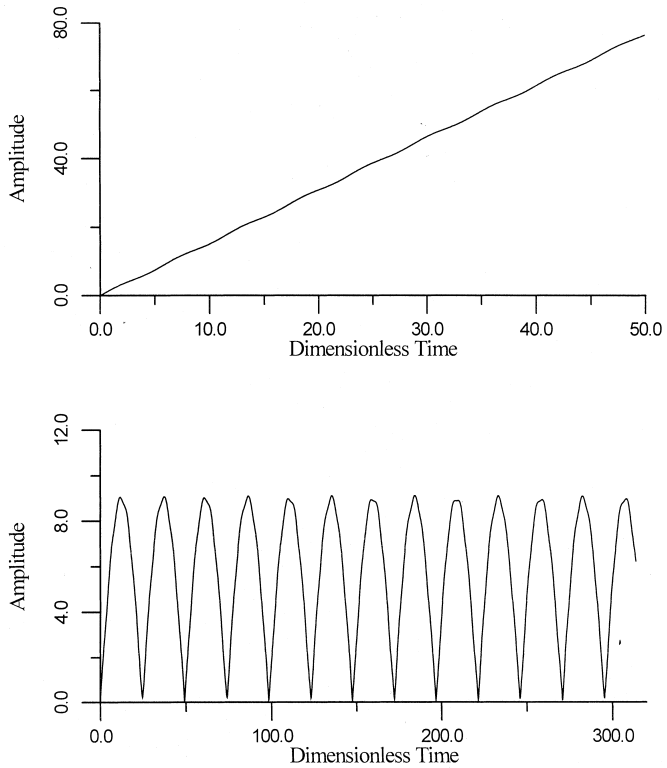

Fig. 10. Time history of the amplitude a_3 for $\hat{M} = 0.5$, $\xi = 0.2$ and $\varepsilon\sigma_3 = -0.4$ ($\omega_3 = 2.4$) (bottom plot) and $\varepsilon\sigma_3 = -0.192$ ($\omega_3 = 2.192$) (top plot).

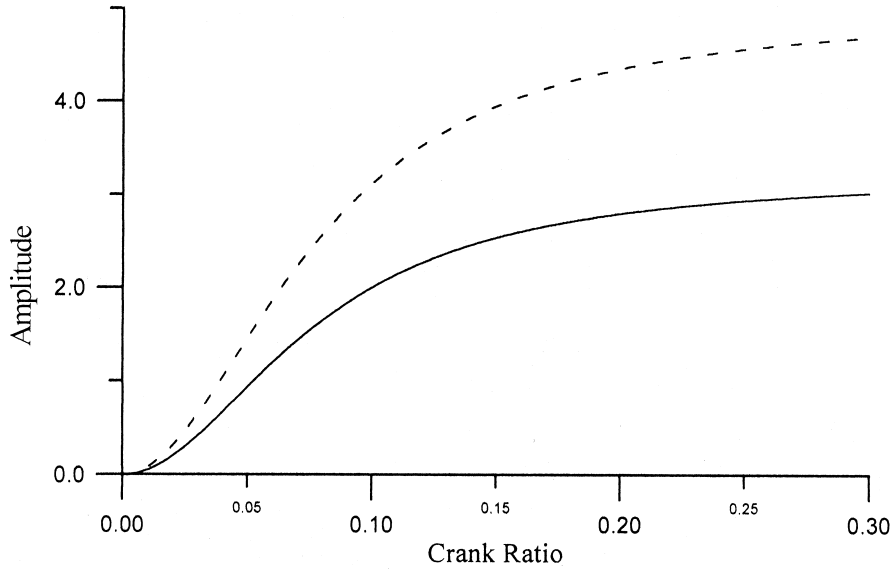

Fig. 11. The amplitude a_3 vs the crank ratio ξ for $\varepsilon\sigma_3 = 0.2$ ($\omega_3 = 1.8$) and $\hat{M} = 0.5$ (solid line) and $\hat{M} = 1.0$ (dashed line).

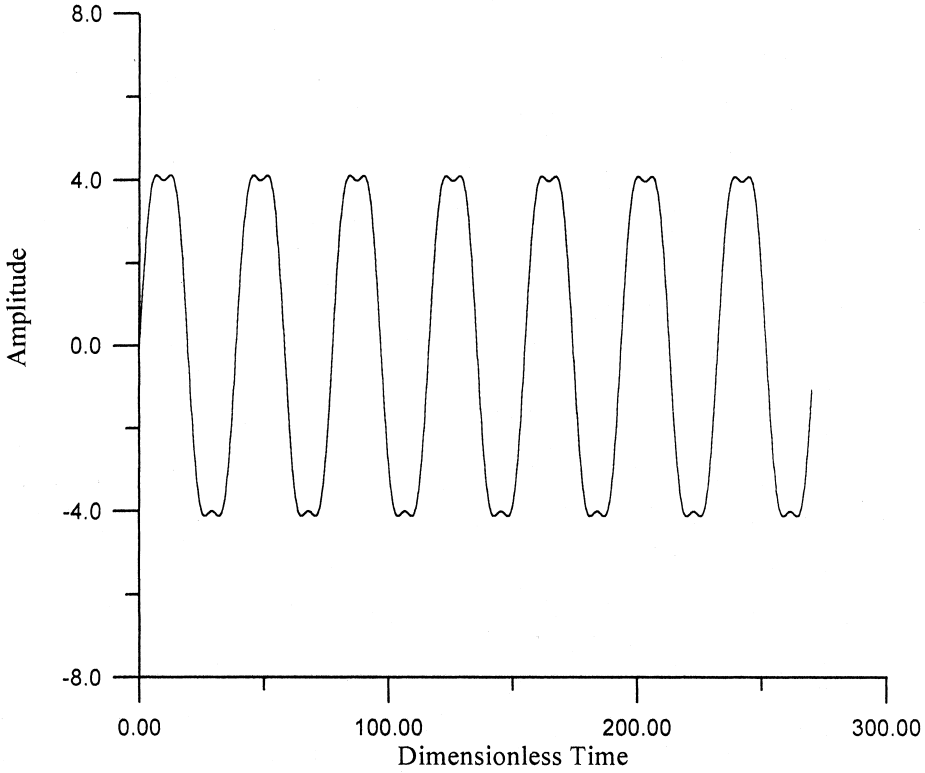

Fig. 12. The long-time behavior of the amplitude a_3 for $\hat{M} = 1.0$, $\varepsilon\sigma_3 = 2$ and $\xi = 0.13$.

Acknowledgement

The work reported here was supported by the National Science Council, Taiwan, under Grant No. NSC86-2212-E-018-001 to the National Chunghua Normal University. The author also wishes to express his appreciation to the reviewers for their constructive suggestions.

Appendix

$$\frac{\partial T(\eta,\tau)}{\partial \eta} = -\xi\cos\tau + 2\xi\cos\tau\sum_{k=1}^{\infty}\dot{A}_k(\tau)\sin k\pi\eta - \xi\sin\tau\sum_{k=1}^{\infty}A_k(\tau)\sin k\pi\eta + \xi^2[\sin^2\tau - (\cos^2\tau)\eta] - \tfrac{1}{2}\xi^3\cos\tau\sin^2\tau$$

$$\begin{aligned} T(\eta,\tau) = {} & -\xi\cos\tau(\eta-1) + \hat{M}\xi\cos\tau - \hat{I}_m\xi\sin\tau\sum_{k=1}^{\infty}(k\pi)^3\cos k\pi\eta|_{\eta=1} \\ & - 2\xi\cos\tau\left(\sum_{k=1}^{\infty}\dot{A}_k(\tau)\int_{\eta}^{1}\sin k\pi\eta\,\mathrm{d}\eta\right) + \xi\sin\tau\left(\sum_{k=1}^{\infty}A_k(\tau)\int_{\eta}^{1}\sin k\pi\eta\,\mathrm{d}\eta\right) \\ & + \xi^2\sin^2\tau(\eta-1) + \hat{M}\xi^2\cos 2\tau - \tfrac{1}{2}\xi^2\cos^2\tau(\eta^2-1) \\ & + \tfrac{1}{2}\xi^3\cos\tau\sin^2\tau(\eta-1) - \tfrac{1}{2}\xi^3\hat{M}\cos\tau\sin^2\tau + \tfrac{1}{2}\xi^3\hat{M}\cos\tau\sin 2\tau \end{aligned}$$

$$\alpha_{ij}^{cs} = \int_0^1(\cos i\pi\eta)\sin j\pi\eta\,\mathrm{d}\eta = \frac{1}{2}\left[\frac{(-1)^{i-j}-1}{(i-j)\pi} - \frac{(-1)^{i+j}-1}{(i+j)\pi}\right](1-\delta_{ij})$$

$$\alpha_{ij}^{\eta ss} = \int_0^1\eta(\sin i\pi\eta)\sin j\pi\eta\,\mathrm{d}\eta = \frac{1}{4}\delta_{ij} + \frac{1}{2}\left[\frac{(-1)^{i-j}-1}{(i-j)\pi} - \frac{(-1)^{i+j}-1}{(i+j)\pi}\right](1-\delta_{ij})$$

where δ_{ij} is the Dirac delta function.

References

Badlani, M., Kleinhenz, W., 1979. Dynamic stability of elastic mechanisms. ASME, Journal of Mechanical Design 101, 149–153.

Badlani, M., Midha, A., 1982. Member initial curvature effects on the elastic slider-crank mechanism response. ASME, Journal of Mechanical Design 104, 159–167.

Beale, D., Lee, S.W., 1996. Nonlinear equation instability boundaries in flexible mechanisms. ASME, Journal of Mechanism and Machine Theory 31, 215–227.

Bolotin, V.V., 1964. The Dynamic Stability of Elastic Systems, Holden–Day.

Chu, S.-C., Pan, K.C., 1975. Dynamic response of a high-speed slider-crank mechanism with an elastic connecting rod. ASME, Journal of Engineering for Industry 97, 542–550.

Halbig, D., Beale, D.G., 1995. Experimental observations of a flexible slider-crank mechanism at very high speed. Nonlinear Dynamics 7, 365–384.

Hsieh, S.R., Shaw, S.W., 1994. Dynamic stability and nonlinear resonance of a flexible connecting rod: single-mode model. Journal of Sound and Vibration 170, 25–49.

Hsu, C.S., 1965. Further results on parametric excitation of a dynamic system. ASME, Journal of Applied Mechanics 87, 373–379.

Jasinski, P.W., Lee, H.C., Sandor, G.N., 1970. Stability and steady-state vibrations in a high-speed slider crank mechanism. ASME, Journal of Applied Mechanics 92, 1069–1076.

Jasinski, P.W., Lee, H.C., Sandor, G.N., 1971. Vibrations of elastic connecting rod of a high-speed slider-crank mechanism. ASME, Journal of Engineering for Industry 93, 636–644.

Meirovitch, L., 1970. Methods of Analytical Dynamics. McGraw-Hill.

Nayfeh, A.H., Mook, D. T., 1979. Nonlinear Oscillations. John Wiley & Sons.

Tadjbakhsh, I.G., 1982. Stability of motion of elastic planar linkages with application to slider crank mechanism. ASME, Journal of Mechanical Design 104, 698–703.

Tadjbakhsh, I.G., Younis, C.J., 1986. Dynamic stability of the flexible connecting rod of a slider crank mechanism. ASME, Journal of Mechanisms, Transmissions, and Automation in Design 108, 487–496.

Viscomi, B.V., Ayre, R.S., 1971. Nonlinear dynamics response of elastic slidercrank mechanism. ASME, Journal of Engineering for Industry 93, 251–267.

Zhu, Z.G., Chen, Y., 1983. The Stability of the Motion of a Connecting Rod. ASME, Journal of Mechanisms, Transmissions and Automation in Design 105, 637–640.